

# Immersion Lens Microscopy of Photonic Nanostructures and Quantum Dots

Bennett B. Goldberg, S. B. Ippolito, *Member, IEEE*, Lukas Novotny, Zhiheng Liu, and M. Selim Ünlü, *Senior Member, IEEE*

*Invited Paper*

**Abstract**—We describe recent experimental and theoretical advances in immersion lens microscopy for both surface and subsurface imaging as applied to photonic nanostructures. We examine in detail the ability of sharp metal tips to enhance local optical fields for nanometer resolution microscopy and spectroscopy. Finally, we describe a new approach to nano-optics, that of combining solid immersion microscopy with tip-enhanced focusing and show how such an approach may lead to 20-nm resolution with unity throughput.

**Index Terms**—Microscopy, nano-optics, nanostructures, near-field.

## I. INTRODUCTION

THE SEMICONDUCTOR industry has continued to advance at the rapid pace of Moore's Law through continued shrinking of the physical dimensions of the semiconductor devices, which are already at the nanoscale and will soon approach the atomic scale. Recent advances have made it possible to assemble materials and components atom by atom, or molecule by molecule, allowing for controlled fabrication of nanostructures with dimensions of from 3 to 100 nm. Compared to the behavior of isolated molecules or bulk materials, the behavior of nanostructures exhibit important physical properties not necessarily predictable from observations of either individual constituents or large ensembles. Predominant at the nanoscale are size confinement and quantum mechanical behavior observed in optical and electronic properties, as well as distinct elastic and/or mechanical features—properties that have yet to be directly observed in many cases, and whose underlying principles require study. In this paper, we describe the application of high-resolution optical microscopy, in particular solid immersion lens microscopy, to the characterization of nanostructures.

Nano-optics addresses the broad spectrum of optics on the nanometer scale covering technology and basic science, spanning nanolithography to high-density optical data storage

Manuscript received June 13, 2002; revised July 31, 2002. This work was supported in part by the Defense Advanced Research Projects Agency Heretic program and in part by the U.S. Army Research Labs.

B. B. Goldberg and Z. Liu are with the Boston University Department of Physics and Photonics Center, Boston, MA 02215 USA.

S. B. Ippolito and M. S. Ünlü are with the Boston University College of Engineering and Photonics Center, Boston, MA 02215 USA.

L. Novotny is with the Institute of Optics, University of Rochester, Rochester, NY 14627 USA.

Digital Object Identifier 10.1109/JSTQE.2002.804232

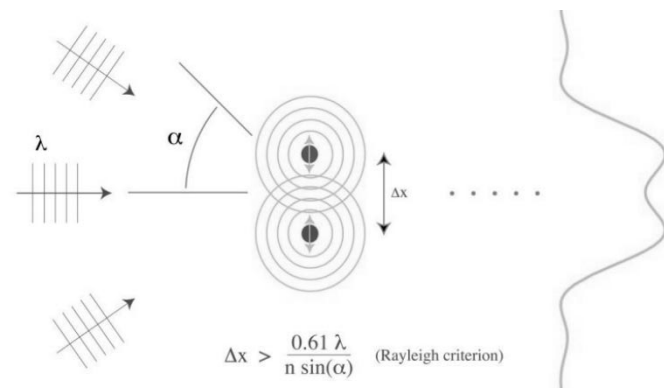


Fig. 1. Schematic representation of Rayleigh criterion showing the minimum detectable separation of two light scatterers for a given optical system.

in technology, and from imaging individual quantum dots (QDs) to atom-photon interactions in the optical near-field in basic physical sciences. Critical to any discussion of optical microscopy and spectroscopy are the fundamental limitations of conventional microscopy. In case of imaging objects with optical fields propagating in the far field, the basic constraint is the diffraction of light, which limits standard optical microscopy to a spatial resolution comparable to half the wavelength of light (see Fig. 1). For imaging objects through a substrate, which is generally opaque for short wavelengths, this limitation becomes more stringent. Imaging guided-wave devices represents even a bigger challenge for conventional microscopy, since light does not couple to the far-field rendering conventional microscopy useless.

Reducing the wavelength or increasing the collected solid angle can improve the spatial resolution of surface microscopy. This has been achieved both with oil immersion and solid immersion lens (SIL) microscopy techniques [1], [2], which reduce the wavelength by immersing the object space in a material with a high refractive index. The large  $n$  in the object space in standard subsurface microscopy of planar samples does not increase the numerical aperture because of refraction at the planar boundary. We have recently developed novel techniques based on a numerical aperture increasing lens (NAIL) [3] to study semiconductors at very high spatial resolution. The techniques we propose below build on both solid immersion and near-field microscopy.

In this paper, we briefly review the basic limitations of standard far-field optical microscopy and recent advances in aperture near-field microscopy. We discuss principles and recent literature in solid-immersion lens microscopy and present our results on subsurface imaging using NAIL. Application of SIL-based microscopy to spectroscopy of QDs is also presented along with the basics of instrumentation. We then discuss theoretical and recent experimental results on an apertureless technique that makes use of the strongly enhanced electric field close to a sharply pointed metal tip under laser illumination, and finally propose a combination of SIL technique with tip enhancement.

## II. SPATIAL RESOLUTION IN FAR-FIELD OPTICAL MICROSCOPY

Diffraction limits standard optical microscopy to a spatial resolution of about half the wavelength of light. Fig. 1 shows schematically how a conventional imaging system resolves two closely spaced points. The Rayleigh criterion for resolution prescribes a minimum distance between the two point objects as proportional to wavelength  $\lambda$  and inversely proportional to numerical aperture [ $\text{NA} = n \sin(\alpha)$ , where  $n$  is the refractive index in the object space and  $\alpha$  is the half-angle subtended]. Higher resolution can be obtained by using shorter wavelengths similar to the use of short-wavelength optical lithography for semiconductor circuit fabrication. In most microscopy and spectroscopy applications, however, the wavelength cannot be arbitrarily selected as it is determined by the optical properties of the materials under study. For example, optical absorption in silicon limits inspection through the substrate to  $\lambda \geq 1 \mu\text{m}$ , yielding a theoretical lateral spatial resolution limit for standard subsurface microscopy of about  $0.5 \mu\text{m}$ .

## III. APERTURE NEAR-FIELD MICROSCOPY

In recent years, a proximal probe, aperture microscopy technique called near-field optical microscopy (NSOM) [4]–[7] has extended the range of optical measurements beyond the diffraction limit and stimulated interests in many disciplines, especially material and biological sciences [8]. Aperture scanning near-field microscopy, first described in the early years of the 1900s [9], is a technique that allows for arbitrarily small details to be resolved by scanning a small aperture over the object. Light can only pass through the aperture, and so the aperture size and its proximity to the object determine the resolution of the system (see Fig. 2).

Near-field optical techniques can be applied to probe complex semiconductor nanostructures as well as individual molecules. Recent NSOM studies of materials and devices have addressed issues of laser diode mode profiling, minority carrier transport, near-field photocurrent response of quantum-well structures and laser diodes, imaging of local waveguide properties, and location and studies of dislocations in semiconductor thin films [10]. NSOM studies of nanostructures have revealed novel optical properties of coupled quantum cubes [11], and self-assembled QDs [12], the super-resolution providing the necessary spatial discrimination. Work on photonic bandgap systems

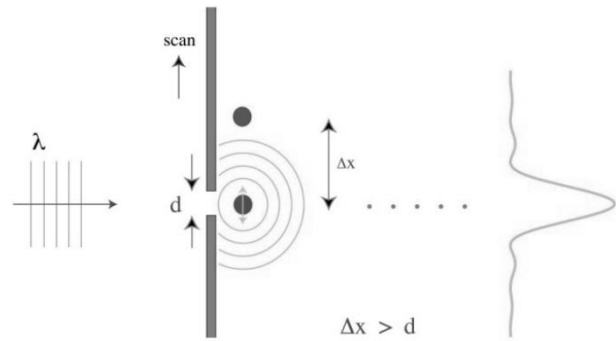


Fig. 2. Schematic of aperture scanning near-field microscopy.

has also continued, striving to image the localized photon states in the bandgap resonance. Studies have also focused on artificial nanostructures, elucidating the plasmon properties of noble metal particles and waveguides [13], [14] and polymer nanoparticles [15].

In the most widely adopted aperture approach [6], [7], light is sent down an aluminum-coated tapered fiber tip of which the foremost end is left uncoated to form a small aperture. Unfortunately, most NSOM probes created by heating and pulling have transmissions of  $\sim 10^{-4}$  due to mode cutoff. The low light throughput and the finite skin depth of the metal are the factors limiting resolution. Furthermore, the input power cannot be increased arbitrarily because a significant fraction of the power is absorbed in the coating and high-power levels result in catastrophic failure of the probe, thus limit the signal-to-noise ratio of small apertures [16]. While NSOM studies with specialized double-tapered probes have overcome some of these limitations [11], [17], we focus our attention in this paper on new solid immersion and apertureless techniques with very large optical throughput.

In general then, near-field microscopy is essentially limited by two factors. First, subwavelength apertures transmit a small fraction ( $10^{-4}$ – $10^{-6}$  for  $a < 100 \text{ nm}$ ) of the incident light; and second, NSOM is by its very nature a serial technique, with relatively slow image acquisition rates. Combined, these factors restrict the utility of NSOM to experiments where proximity of the probe provides new information (see photonic nanostructures below), and where the source is bright, largely time independent and long lived. As a result, time resolved, pump probe, Raman, and nonlinear spectroscopies are not widespread.

## IV. SOLID IMMERSION LENS MICROSCOPY

SIL microscopy [1] improves resolution without the huge loss of light associated with NSOM through the use of a semispherical lens of high index. For some applications such as quantum-dot characterization, the SIL can significantly improve the light collection efficiency beyond that of conventional optical microscopy. This makes it especially attractive for spectroscopy of quantum structures, where both high resolution and large light collection efficiency are requirements. In addition, when the hemisphere is index matched to a substrate material, SIL microscopy provides special imaging capabilities for subsurface microscopy, which we demonstrate with silicon integrated circuit metrology.

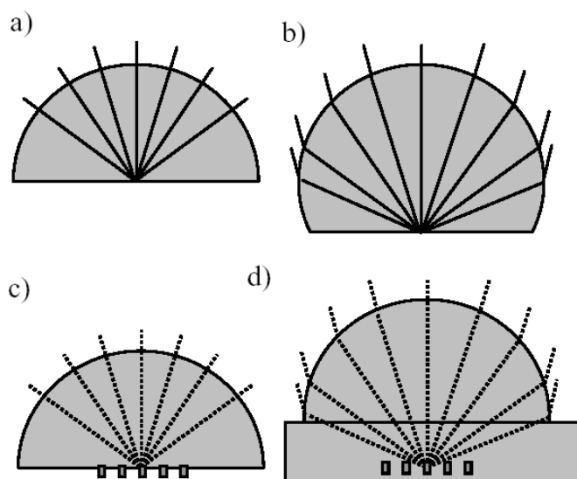


Fig. 3. Solid immersion lens configurations. In (a), a hemispherical lens increases resolution by  $\sim n$ . (b) A Weierstrass optic, or super-SIL, has a resolution increase of  $\sim n^2$ . Two types of imaging modes, surface solid immersion microscopy (c) and subsurface SIM in (d).

The SIL is a solid plano-convex lens of high refractive index that provides an optimum focus of a Gaussian beam. There are two configurations with a semispherical lens that achieve diffraction-limited performance. One focus exists at the center of the sphere, with incoming rays perpendicular to the surface and is generally termed an SIL [1] (see Fig. 3). Also, a second focus exists at a set of aplanatic points [18] a distance  $R/n$  below the center of the sphere, and whose rays are refracted at the spherical surface. This type is generally referred to as a super-SIL [19], or Weierstrass optic [23]. While the super-SIL configuration has a greater magnification ( $n^2$  versus  $n$ ) and increased numerical aperture, it suffers from strong chromatic aberration. The applications of solid immersion microscopy fall into two categories: surface [1] and subsurface imaging [3], [20]. In the latter, the SIL (or super-SIL) is used to image objects below the lens and into the sample under study. In this case of subsurface imaging, a good match in index between the lens and substrate must be maintained. SIL microscopy was originally envisioned for optical data storage [21], but has recently seen several important physics [22] and nanoimaging [23], [24] applications [25]–[27].

Solid immersion lenses exploit the existence of a significant amount of light above the critical angle for the high resolution and large collection efficiency. This leads to a unique aspect of surface SIM: When the optical index of the investigated object is smaller than that of the lens material, as is usually the case of most materials, then the plane wave components of the focused wave undergo total internal reflection when impinging the SIL/object interface above critical angle. Total internal reflection (TIR) produces local evanescent waves in the vicinity of the focal point, an aspect that is often put forward in the literature as extending SIM to near-field optical microscopy. However, TIR is also accompanied with an inseparable combination of more subtle phenomena which stem from the slower wave propagation velocity in the SIL material. In solid-state systems, this is referred to as the Goos–Hänchen reflected beam displacement and has an analogy in geological sciences called v. Schmidt’s lateral waves [2]. In the Goos–Hänchen effect,

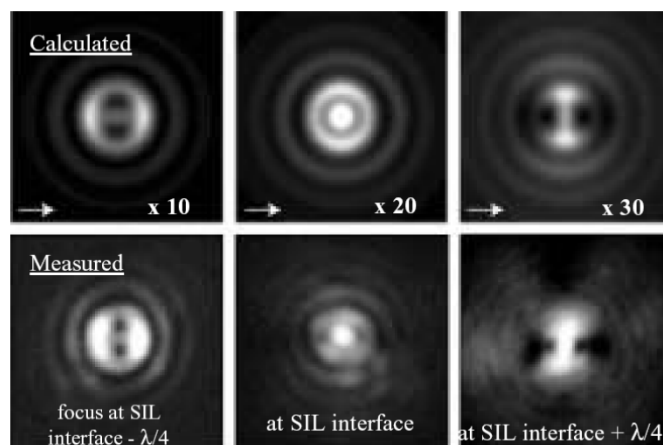


Fig. 4. Comparison of experiment and theory demonstrating the aberrations due to the Goos–Hänchen reflected beam displacement. The upper panel are calculations and the lower measured. The arrows indicate polarization, and the multipliers the relative size of the image.

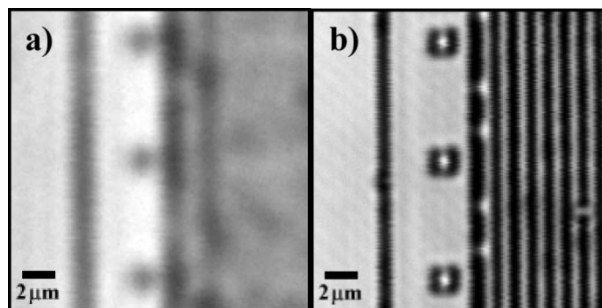


Fig. 5. (a) Lateral line scans of a periodic structure with a spatial frequency of  $s = 0.4 \mu\text{m}^{-1}$ . (b) Measured values and theoretical function of the modulation transfer function plotted by normalized defocus values.

the photons that are tunneling into the less optically dense object medium reemerge into the SIL laterally displaced from impinging point. This produces a lateral beam shift of the total internal reflected plane wave components. The v. Schmidt’s lateral waves, well known in seismology, trails the diverging reflected wave components originating from the focused spot in the form of a conical wave front in a way similar to the Mach cone in fluid dynamics.

We have found that indeed such TIR-related effects lead to a sizable aberration in the image formation of the focused spot. We have demonstrated that luckily this aberration does not affect the *actual size* of the probing focused spot. Furthermore, it can be used in conjunction with confocal microscopy in order to greatly enhance the reflected image contrast of low optical index objects. Fig. 4 displays a comparison of theory and experiment of the image of a tightly focused spot at the interface between a high-index SIL and a low-index medium. The results of both indicate that a significant fraction of optical power reflected from the interface is laterally displaced; thus, a confocal arrangement yields higher than expected contrast with lower than expected reflected power. Similarly, the probing spot as defined by the incident waves is tightly focused, as expected [2].

When imaging below the planar surface of a sample, refraction prevents a conventional optical microscope from operating

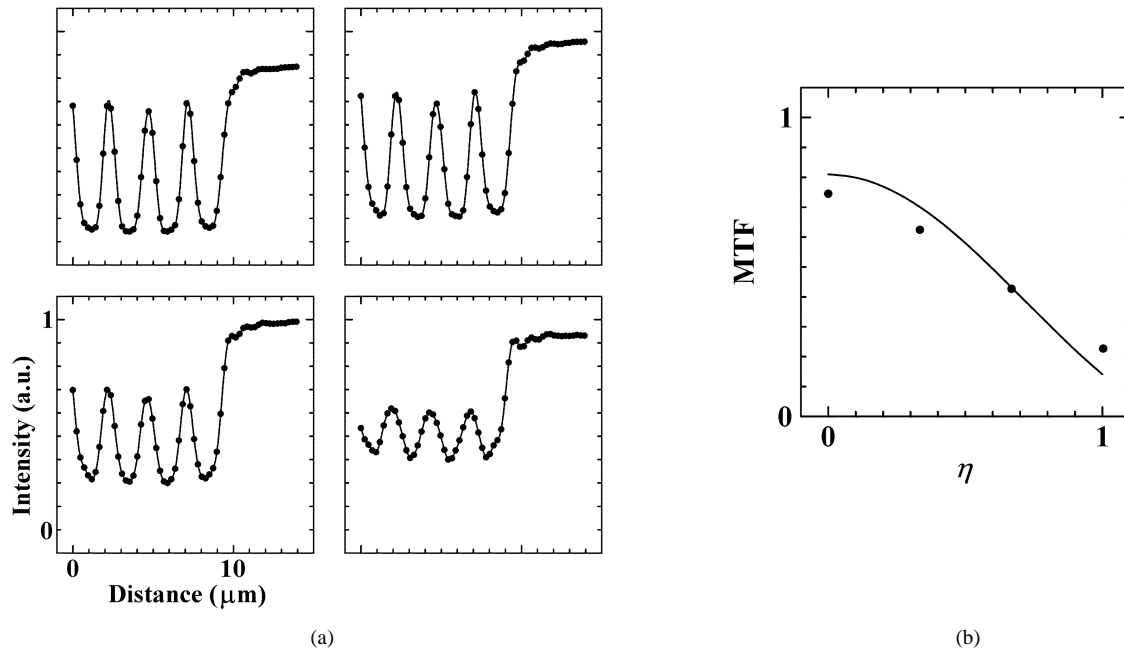


Fig. 6. Through substrate imaging of a silicon IC using an AMOS-200 IC failure analysis system demonstrating the improvement in longitudinal resolution. (a) Line scans of periodic  $0.4 \mu\text{m}$  periodic structures with defocus steps of  $1 \mu\text{m}$ . (b) Modulation transfer function showing close to diffraction limited performance.

with a resolution near the diffraction limit. The spatial resolution is not improved by the larger index of the material because light cannot be externally coupled beyond the critical angle. By adding a lens to the backside planar surface of the sample this light can be externally coupled, yielding improved resolution and larger collection efficiency. The imaging quality is greatly improved over that of the surface SIL, because the interface is out of focus. This is the second, subsurface configuration referred to above. We have demonstrated the improvement in resolution that the lens provides by inspection of silicon integrated circuits through the substrate [3] (see Fig. 5).

Though the lateral spatial resolution can be evaluated from a lateral intensity distribution, the dielectric interfaces in the vertical, or longitudinal direction, create a complicated transfer function that does not facilitate a simple evaluation of the longitudinal spatial resolution. By measuring the modulation transfer function (MTF)—the ratio of object to image contrast—of a laterally periodic structure with longitudinal defocusing, we can test the longitudinal spatial resolution [28]. A line scan of a periodic structure with a spatial frequency of  $s = 0.4 \mu\text{m}^{-1}$  is shown in Fig. 6. The resulting normalized spatial frequency  $\nu = s \cdot \lambda_0 / NA = 0.3$ . Defocusing the sample by  $\Delta z$  increments of  $1 \mu\text{m}$  translates into normalized defocus increments of  $\eta = \Delta z \cdot NA^2 / (2 \cdot \lambda_0 \cdot n) = 0.33$ . The experimentally measured MTF values are compared to the MTF function the optical system would exhibit if it were diffraction limited in Fig. 6. The decay in coupling of this spatial frequency indicates the system is close to diffraction limited. With the  $5\times$  microscope objective lens and NAIL we have  $\sim 1.3 \mu\text{m}$  longitudinal spatial resolution, whereas a  $100\times$  microscope objective lens has  $\sim 12 \mu\text{m}$  longitudinal spatial resolution. The spatial resolution improvement laterally is at least a factor of 3.5 while longitudinally it is at least a factor of 12.5. The greatest longitudinal resolution is 280 nm, which would allow vertical sectioning of an integrated circuit's layer structure.

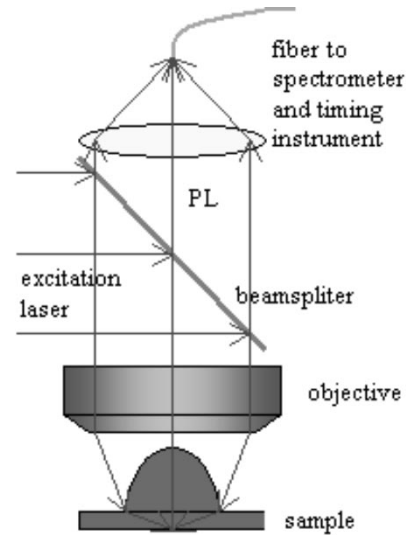


Fig. 7. Schematic of confocal microscope combined with solid immersion NAIL technique. The QDs are excited and the PL collected through the backside of the sample. The NAIL and the substrate of the sample are in optimal optical contact to ensure maximum transmission at large angles.

## V. NANOSCALE QUANTUM-DOT SPECTROSCOPY

QDs have received an enormous amount of interest in recent years because they serve as an excellent new system to study basic quantum physics with engineered atomic-like properties [29]–[32]. Coherence, coupling, carrier dynamics and other fundamental properties are only accessible when individual dots are examined experimentally [33], [34]. For a self-assembled QD sample, the typical QD size is  $\sim 20 \text{ nm}$  and areal QD density is  $10^8 \sim 10^{10} / \text{cm}^2$ . So to excite just a few dots within a small spectral window, the sample area under investigation must be reduced to a few hundred nanometers in size. To accomplish this, one approach is aperturing or focusing the excitation laser tightly to a spot size of that magnitude [22], [35], [36]. Another

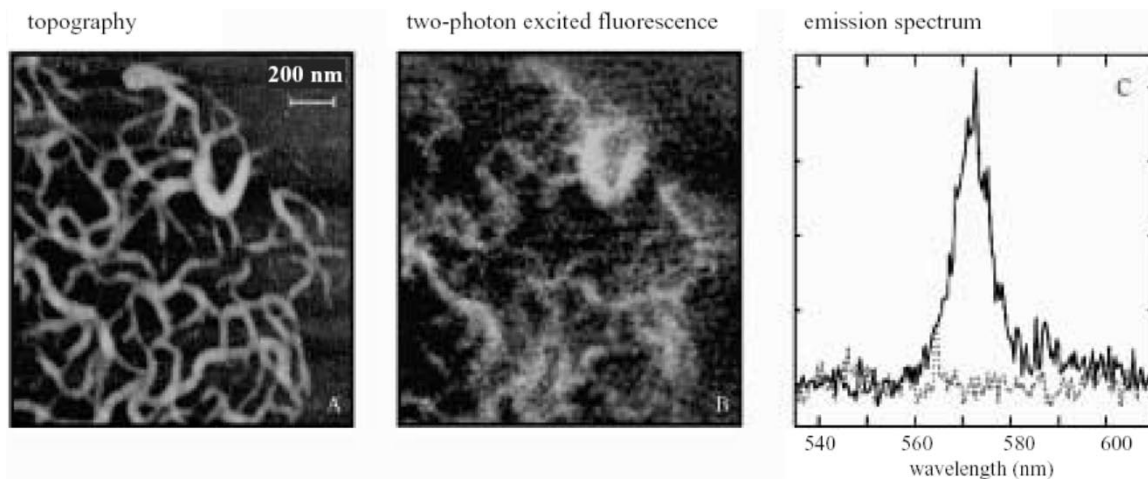


Fig. 8. Simultaneous topographic image (A) and near-field two-photon excited fluorescence image (B) of J-aggregates of PIC dye in a PVS film on a glass substrate. (C) Corresponding fluorescence emission spectrum obtained with (solid line) and without (dashed line) the tip present.

approach is creating a mask or etching a mesa on the sample itself [30], [37]. The latter technique has the major drawback that spatial scanning and spectral imaging cannot be performed and, thus, the interactions between neighboring dots, diffusion, wave function spatial structure, and other optical properties cannot be investigated. Here, we will address the former method in additional detail.

Near-field scanning optical microscopy (NSOM) has been used to probe a small number of QDs. Saiki's group used NSOM to investigate the homogeneous linewidth broadening of single InGaAs QD at room temperature with a spatial resolution of 250 nm, which is determined by the aperture diameter of NSOM tip [35]. For the past five years, our group has used NSOM to investigate the physics of self-assembled QDs (SADs) at low temperature. The resolution provided by NSOM allows the interrogation of individual QDs, even in the density regime where dot-to-dot coupling occurs. We have studied pressure-induced strain tuning of individual QDs [36], observation and mapping of spectral diffusion in individual QDs [38], and examined interdot coupling [12], likely due to extended hole states [39].

However, the throughput of NSOM is low and cryogenic NSOM experiments complex. Solid immersion microscopic techniques have been developed to overcome these limitations of NSOM but still provide similar ultrahigh spatial resolution [23], [27], [40]. Grober's group has implemented solid immersion lens in imaging spectroscopy of quantum well and QDs, achieving a spatial resolution of 240 nm [40].

Our group is utilizing backside immersion microscopy (NAIL technique, see Section III [3]) and scanning confocal microscopy to investigate the physics of InGaAs QDs, especially the dynamics of excitons in QDs [41], decoherence [42], and coupling between QDs [32] (see Fig. 7). The numeric aperture of the system is increased by  $\sim n^2 = 13$  achieving a spatial resolution of  $\sim 120$  nm. Due to the high NA of our system, the collection efficiency will be large enough to perform time resolved PL experiments as well pump-probe experiments on individual dots without resorting to aperture, mask, or etched mesa techniques.

## VI. TIP-ENHANCED NEAR-FIELD OPTICAL MICROSCOPY

In aperture-type near-field optical microscopy, light is sent down an aluminum-coated fiber tip of which the foremost end is left uncoated to form a small aperture [6]. Unfortunately, only a tiny fraction of the light coupled into the fiber is emitted through the aperture because of the cutoff of propagation of the waveguide modes [16]. The low light throughput and the finite skin depth of the metal are the limiting factors for resolution. Nowadays, it is doubted that an artifact-free resolution of 50 nm will be surpassed by the aperture technique. However, many applications in nanotechnology require higher spatial resolutions.

Recently, a new apertureless technique has been introduced to overcome the limitations of aperture probes [43], [44]. The technique makes use of the strongly enhanced electric field close to a sharply pointed metal tip under laser illumination. The energy density close to the metal tip can be strongly increased over the energy density of the illuminating laser light. The tip is held a few nanometers above the sample surface so that a highly localized interaction between the enhanced field and the sample is achieved. In order to obtain a high image contrast, nonlinear optical interactions based on multiphoton processes have been used. With this technique, spectroscopic measurements with spatial optical resolutions on the order of 10 nm have been achieved [44]. To date, this is the highest reported spatial resolution of a spectroscopic measurement (see Fig. 8).

The use of laser-illuminated metal tips for near-field imaging has been discussed by many groups but most of the work has been limited to light scattering at the metal tip. The tip locally perturbs the fields at the sample surface; the response to this perturbation is detected in the far-field at the same frequency of the incident light. Homodyne detection using lock-in techniques is commonly applied to discriminate the signal against the background. Interference with a reference field has been introduced to increase the contrast and it has been demonstrated that more specific information can be extracted by detecting the scattering signal at higher harmonics of the vibration frequency. In general, the detected signals contain both near-field and far-field contributions, and often are dominated by topographic rather than

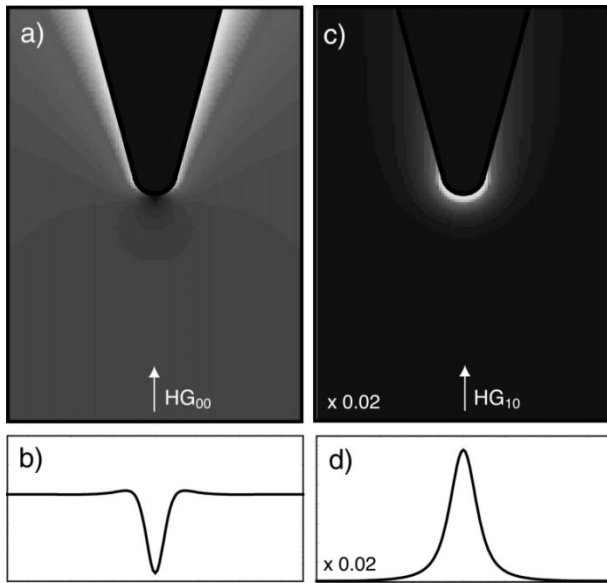


Fig. 9. Calculated near-field of a gold tip (5-nm tip radius) irradiated at  $\lambda = 810$  nm with two different focused laser modes along the tip axis. (a), (b) Gaussian laser mode, and (c), (d) Hermite–Gaussian (1,0) mode. (a), (c) show plots of the electric field intensity ( $E^2$ ) and (b), (d) are linecuts of (a), (c) evaluated on a transverse line 1 nm beneath the tip. The field enhancement is driven by the electric field polarized along the tip axis (longitudinal field). This field is zero for an on-axis Gaussian laser mode whereas it can become stronger than the transverse field for a  $HG_{10}$  mode. Calculations based on the MMP method [46].

spectroscopic information. The interpretation of the contrast in the recorded images is therefore difficult.

Instead of using the metal tip as a local scatterer, it can also be used as a local light source if proper polarization and excitation conditions are met. The field near the tip apex can become strongly enhanced over the field of the illuminating laser light thereby establishing a nanoscopic light-source [45]. Thus, instead of using a tip to locally scatter the sample's near-field, the tip is used to provide a local excitation source for a spectroscopic response of the sample [44]. This approach enables simultaneous *spectral* and subdiffraction *spatial* measurements, but it depends sensitively on the magnitude of the field enhancement factor. The latter is a function of wavelength, material, geometry, and polarization of the exciting light field. Although theoretical investigations have led to a wide range of values for the field enhancement factor these studies are consistent with respect to polarization conditions and local field distributions.

Fig. 9 shows the field distribution near a sharp gold tip in water irradiated by two different monochromatic plane-wave excitations calculated by the multiple multipole (MMP) method [46]. The wavelength of the illuminating light is  $\lambda = 810$  nm and the corresponding dielectric constant of gold tip is  $\epsilon = -24.9 + 1.57i$ . In Fig. 9(a), the tip is irradiated from the bottom by an on-axis fundamental Gaussian beam for which the polarization is perpendicular to the tip axis. On the other hand, in Fig. 9(c) the tip is irradiated by a focused, on-axis Hermite-Gaussian (1,0) mode which possesses a strong longitudinal field at the center of its focus [47]. Fig. 9(b) and (d) show corresponding cuts along a transverse line 1 nm beneath the tip. A striking difference is seen for the two different excitations: in Fig. 9(c), the intensity near the tip end is strongly increased over the illuminating intensity,

whereas no enhancement beneath the tip exists in Fig. 9(a). This result suggests that it is crucial to have a large component of the excitation field along the axial direction to obtain a high field enhancement. Calculations of platinum and tungsten tips show lower enhancements, whereas the field beneath a dielectric tip is reduced compared to the excitation field.

The incident light drives the free electrons in the metal along the direction of polarization. While the charge density is zero inside the metal at any instant of time ( $\text{div } \mathbf{E} = 0$ ), charges accumulate on the surface of the metal. When the incident polarization is perpendicular to the tip axis, diametrically opposed points on the tip surface have opposite charges. As a consequence, the foremost end of the tip remains uncharged. On the other hand, when the incident polarization is parallel to the tip axis, the induced surface charge density is rotationally symmetric and has the highest amplitude at the end of the tip. In both cases, the surface charges form an oscillating standing wave (surface plasmons) with wavelengths shorter than the wavelength of the illuminating light indicating that it is essential to include retardation in the analysis.

The magnitude of the field enhancement factor is crucial for imaging applications. The direct illumination of the sample surface gives rise to a far-field background signal. If we consider an optical interaction that is based on a  $n$ th-order nonlinear process and assume that only the sample surface is active, then the far-field background will be proportional to

$$S_{ff} \sim AI_o^n$$

where  $A$  is the illuminated surface area and  $I_o$  is the laser intensity. The signal that we wish to detect and investigate (near-field signal) is excited by the enhanced field at the tip. If we designate the enhancement factor for the electric field intensity ( $E$ ) by  $f_e$  then the near-field signal of interest is proportional to

$$S_{nf} \sim a(f_e^2 I_o)^n$$

where  $a$  is a reduced area given by the tip size. If we require that the signal be stronger than the background ( $S_{nf}/S_{ff} > 1$ ) and use realistic numbers for the areas [ $a = (10 \text{ nm})^2$ ,  $A = (500 \text{ nm})^2$ ] then we find that an enhancement factor of

$$f_e > [2500]^{1/2n}$$

is required. For a first-order process ( $n = 1$ ) such as scattering or fluorescence, an enhancement factor of 50 is required which is beyond the calculated values. Therefore, it is necessary to involve higher order nonlinear processes. For a second-order nonlinear process, the required enhancement factor is only 7. This is the reason why the first experiments have been performed with two-photon excitation [44]. To maximize the field enhancement, various alternative probe shapes and materials have been proposed. It has been determined that finite-sized elongated shapes exhibit very low radiation damping and, therefore, provide very high enhancement factors [48], [49]. Even stronger enhancements are found for tetrahedral shapes [50].

In fluorescence studies, the enhanced field is used to locally excite the sample under investigation to a higher electronic state or band. Image formation is based on the subsequent fluorescence emission. However, the fluorescence can be quenched by the presence of the probe, i.e., the excitation energy can be transferred to the probe and be dissipated through various channels

into heat [51]. Thus, there is a competition between field enhancement and fluorescence quenching. The nonradiative energy transfer rate from molecule to the tip depends on the inverse sixth power of the distance  $d$  between tip and molecule, similar to the case of Förster energy transfer. However, the excitation rate of the molecule also depends on  $d^{-6}$ , since it is proportional to the square of the electric near-field. Hence, for small distances from the tip, there should be no distance dependence of the fluorescence rate of a single molecule if excited by a single photon. Of course, this is a rough estimate and more accurate calculations are needed to understand the interplay between field enhancement and quenching.

While quenching is an issue in fluorescence imaging, there are various applications in near-field optics that are not sensitive to such a competing process. For example, we believe that the combination of field enhancement and nonlinear optical interactions is very promising for technological applications, such as semiconductor mask inspection and lithography. In the past, it has been proposed to perform nanolithography with the sharp tip of an atomic force microscope. However, this is an intrusive technique since it is based on a mechanical interaction between probe and sample. The optical tip-enhanced technique should be able to achieve comparable resolution, and since it is based on an optical interaction, it does not require a physical contact between probe and sample. Since the optical writing in most photoresists is based on nonlinear processes, the prerequisites for this technique are readily met. Furthermore, the technique benefits strongly from the existing knowledge of conventional optical lithography.

Optical data storage based on a solid immersion lens (SIL) has proven to be a fast technique since it does not rely on piezo-positioning. Instead, a constant tip-sample distance is maintained by the air cushion formed between the end-face of the SIL and the rotating sample surface. In the past, we have analyzed the focusing capabilities of SILs [2] and determined the polarization properties. To study the effect of local field enhancement in combination with SIL, we carried out rigorous calculations based on Maxwell's equations using the MMP method [46]. An example of these results is shown in Fig. 10. A radially polarized laser beam is focused on the interface of an optical element with a flat surface. A tip-shaped aluminum particle is placed in close proximity to the surface of the optical element. The end diameter of the tip-shaped particle is 10 nm and the distance to the surface of the optical element is 5 nm. The incoming radially polarized laser light has a wavelength of 800 nm. The figure shows contour lines of constant electric field intensity on a logarithmic scale. The linecuts below Fig. 10(c) represent the electric field intensity 1 nm above the surface of the optical element for the case with and without the tip-shaped particle. This figure demonstrates the much smaller spotsize that can be achieved by using a small structure to enhance the fields. In this particular example, the optical data density can be increased by roughly a factor of 900.

Fig. 11 shows schematically the practical implementation of a tip-enhanced solid immersion lens (TESIL). The metal tip is replaced by a favorably shaped particle located close to the SIL's planar surface and irradiated by a radially polarized laser beam which provides the necessary polarization conditions.

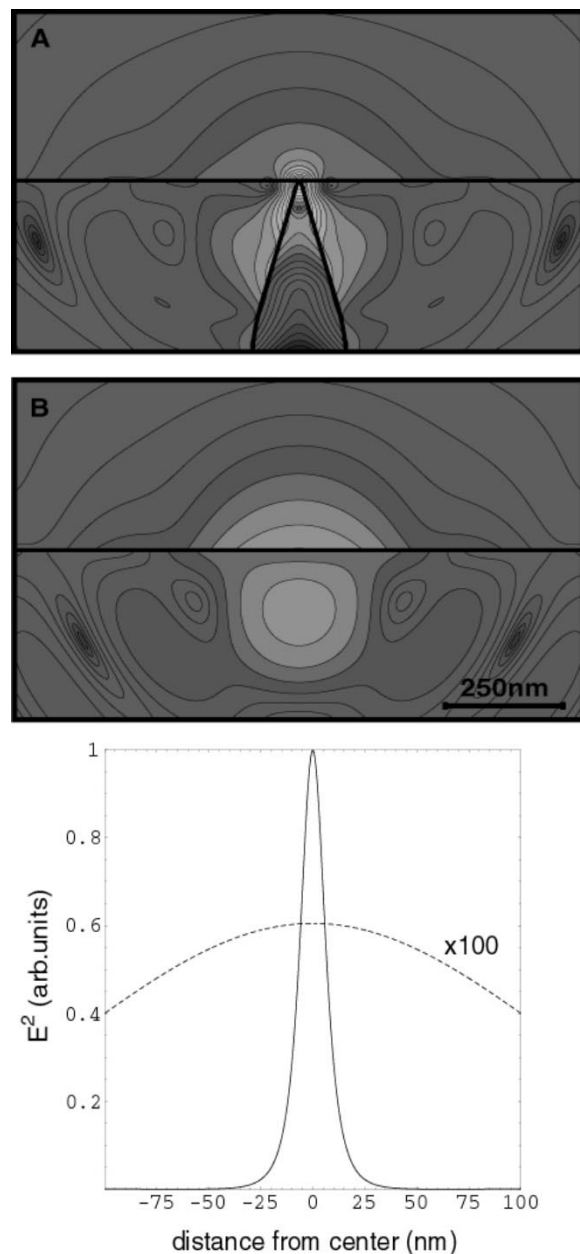


Fig. 10. Calculated field distribution ( $E^2$ , factor of 2 between adjacent contour lines) for a focused, radially polarized laser beam incident on a dielectric/air interface: (A) with a tip-like aluminum particle close to the interface, (B) without the particle. The boundaries between different media are indicated by solid lines. The metal tip attracts the fields and concentrates them toward the interface. The following parameters were used: wavelength = 800 nm, numerical aperture = 1.789, dielectric constant of lower space = 3.2, dielectric constant of upper space = 1, dielectric constant of aluminum tip =  $-24.1 + i 1.5$ , end diameter of tip = 10 nm, distance of tip from interface = 5 nm. (C) Fields evaluated 1 nm above the interface with (solid line) and without (dashed line) the metal tip. The peak field strength for the case with tip is  $\sim 165$  times stronger than without the tip. The full-width at half-maximum (FWHM) with tip is on the order of the tip diameter (10 nm), without a tip the diffraction limited spot is  $\sim 300$  nm.

The TESIL is built using conventional silicon microfabrication. First, SIL lenses are bonded on the back surface of a 100- $\mu\text{m}$  silicon wafer, and a thin layer of resist is deposited on the front surface of the wafer. A small hole (or holes) is made in the resist by an electron or ion beam. After metal deposition and removal of the resist, the small resulting metal particle is

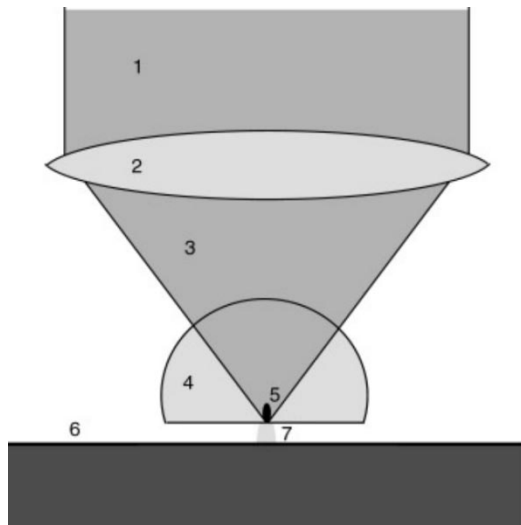


Fig. 11. Combination of SIL with local field enhancement. (1) Incoming laser light with a mode profile that provides an electric field in its focal region perpendicular to the surface of the optical element, (2) focusing lens, (3) focused laser light, (4) optical element, (5) small structure able to locally enhance the electric field of the incoming laser light, (6) sample surface to be optically interacted with, and (7) localized optical interaction.

protected by a silicon nitride coating. The concept extends to parallel imaging. With a grid of particles of separation greater than half a wavelength, conventional beam-steering methods could be used to address the particles one at a time, or multiple beams could be used for faster read/write.

## VII. CONCLUSION

Recent experimental and theoretical advances in immersion lens microscopy has identified the physical basis for the reflectivity of a tightly focused spot at an immersion lens interface, and shown how subsurface imaging can fully utilize the properties of a super-SIL for silicon IC inspection. An interesting application of the NAII is high-resolution, high collection for the spectroscopic study of QDs. In the area of tip-enhanced optical fields, we have addressed the main issues regarding necessary excitation power to lead to our new implementation of combining an SIL with tip-enhanced optical fields. In this later case, we project nanometer-scale lateral resolution for unity throughput, a goal unreachable by any other means of which we are aware.

## ACKNOWLEDGMENT

The authors wish to thank K. Karrai for contributions to this work.

## REFERENCES

- [1] S. M. Mansfield and G. S. Kino, "Solid immersion microscope," *Appl. Phys. Lett.*, vol. 57, pp. 2615–2616, 1990.
- [2] K. Karrai, X. Lorenz, and L. Novotny, "Enhanced reflectivity contrast in confocal solid immersion lens microscopy," *Appl. Phys. Lett.*, vol. 77, pp. 3459–3461, 2000.
- [3] S. B. Ippolito, B. B. Goldberg, and M. S. Ünlü, "High spatial resolution subsurface microscopy," *Appl. Phys. Lett.*, vol. 78, pp. 4071–4073, 2001.
- [4] D. W. Pohl, W. Denk, and M. Lanz, "Optical stethoscopy: Image recording with resolution  $\lambda/20$ ," *Appl. Phys. Lett.*, vol. 44, pp. 651–653, 1984.
- [5] A. Lewis, M. Isaacson, A. Harootunian, and A. Muray, "Development of a 500Å resolution light microscope," *Ultramicroscopy*, vol. 13, pp. 227–231, 1984.
- [6] E. Betzig and J. K. Trautman, "Near-field optics: Microscopy, spectroscopy, and surface modification beyond the diffraction limit," *Science*, vol. 257, pp. 189–195, 1992.
- [7] E. Betzig, A. Lewis, A. Harootunian, M. Isaacson, and E. Kratschmer, "Near-field scanning optical microscopy (NSOM): Development and biophysical applications," *Biophys. J.*, vol. 49, pp. 268–279, 1986.
- [8] For a recent review, see: B. Dunn, "Near-field scanning optical microscopy," *Chem. Rev.*, vol. 99, pp. 2891–2928, 1999.
- [9] E. H. Syngne, "A suggested method for extending microscopic resolution into the ultra-microscopic region," *Phil. Mag.*, vol. 6, pp. 356–362, 1928.
- [10] J. W. P. Hsu, "Near-field scanning optical microscopy of electronic and photonic materials and devices," *Mater. Sci. Eng.*, vol. 33, pp. 1–50, 2001.
- [11] T. Kawazoe, K. Kobayashi, J. Lim, Y. Narita, and M. Ohtsu, "Direct observation of optically forbidden energy transfer between CuCl quantum cubes via near-field optical spectroscopy," *Phys. Rev. Lett.*, vol. 88, p. 067 404, 2002.
- [12] H. D. Robinson, B. B. Goldberg, and J. L. Merz, "Observation of excitation transfer among neighboring quantum dots," *Phys. Rev. B.*, vol. 64, p. 075 308, 2001.
- [13] J. R. Krenn, A. Dereux, J. C. Weeber, E. Bourillot, Y. Lacroute, J. P. Gouffonnet, G. Schider, W. Gotschy, A. Leitner, F. R. Aussenegg, and C. Girard, "Squeezing the optical near-field zone by plasmon coupling of metallic nanoparticles," *Phys. Rev. Lett.*, vol. 82, pp. 2590–2593, 1999.
- [14] M. Salerno, N. Félidj, J. R. Krenn, A. Leitner, F. R. Aussenegg, and J. C. Weeber, "Near-field optical response of a two-dimensional grating of gold nanoparticles," *Phys. Rev. B*, vol. 63, p. 165 422, 2001.
- [15] Y. Shen, D. Jakubczyk, F. Xu, J. Swiatkiewicz, P. N. Prasad, and B. A. Reinhardt, "Two-photon fluorescence imaging and spectroscopy of nanostructured organic materials using a photon scanning tunneling microscope," *Appl. Phys. Lett.*, vol. 76, pp. 1–3, 2000.
- [16] L. Novotny and D. W. Pohl, "Light propagation in scanning near-field optical microscopy," in *Photons and Local Probes*, O. Marti and R. Moeller, Eds. Norwell, MA: Kluwer, 1995, NATO ASI Series, pp. 21–23.
- [17] S.-K. Eah, W. Jhe, and Y. Arakawa, "Near-field optical photoluminescence microscopy of high-density InAs/GaAs single quantum dots," *Appl. Phys. Lett.*, vol. 80, pp. 2779–2781, 2002.
- [18] M. Born and E. Wolf, *Principles of Optics*, 7th expanded ed. Cambridge, U.K.: Cambridge Univ. Press, 1999, p. 159.
- [19] B. D. Terris, H. J. Mamin, D. Rugar, W. R. Studenmund, and G. S. Kino, "Near-field optical data storage using a solid immersion lens," *Appl. Phys. Lett.*, vol. 65, pp. 388–390, 1994.
- [20] S. M. Mansfield, W. R. Studenmund, G. S. Kino, and K. Osato, "High-numerical-aperture lens system for optical storage," *Opt. Lett.*, vol. 18, pp. 305–307, 1993.
- [21] B. D. Terris, H. J. Mamin, and D. Rugar, "Near-field optical data storage," *Appl. Phys. Lett.*, vol. 68, pp. 141–143, 1996.
- [22] Q. Wu, R. D. Grober, D. Gammon, and D. S. Katzer, "Imaging spectroscopy of two-dimensional excitons in a narrow GaAs/AlGaAs quantum well," *Phys. Rev. Lett.*, vol. 83, pp. 2652–2655, 1999.
- [23] M. Yoshita, T. Sasaki, M. Baba, and H. Akiyama, "Application of solid immersion lens to high-spatial resolution photoluminescence imaging of GaAs quantum wells at low temperatures," *Appl. Phys. Lett.*, vol. 73, pp. 635–637, 1998.
- [24] K. Koyama, M. Yoshita, M. Baba, T. Suemoto, and H. Akiyama, "High collection efficiency in fluorescence microscopy with a solid immersion lens," *Appl. Phys. Lett.*, vol. 75, pp. 1667–1669, 1999.
- [25] L. P. Ghislain and V. B. Elings, "Near-field scanning solid immersion microscope," *Appl. Phys. Lett.*, vol. 72, pp. 2779–2781, 1998.
- [26] L. P. Ghislain, V. B. Elings, K. B. Crozier, S. R. Manalis, S. C. Minne, K. Wilder, G. S. Kino, and C. F. Quate, "Near-field photolithography with a solid immersion lens," *Appl. Phys. Lett.*, vol. 74, pp. 501–503, 1999.
- [27] M. Vollmer, H. Giessen, W. Stolz, W. W. Rühle, L. Ghislain, and V. Elings, "Ultrafast nonlinear subwavelength solid immersion spectroscopy at  $T = 8$  K," *Appl. Phys. Lett.*, vol. 74, pp. 1791–1793, 1999.
- [28] T. L. Williams, *The Optical Transfer Function of Imaging Systems, Optics and Optoelectronics Series*. Bristol, U.K.: Institute of Physics, 1999, p. 448.
- [29] D. Gammon, "Electrons in artificial atoms," *Nature*, vol. 405, pp. 899–900, 2000.
- [30] N. H. Bonadeo, J. Erland, D. Gammon, D. Park, D. S. Katzer, and D. G. Steel, "Coherent optical control of the quantum state of a single quantum dot," *Science*, vol. 282, pp. 1473–1476, 1998.

- [31] P. Hawrylak, "Excitonic artificial atoms: Engineering optical properties of quantum dots," *Phys. Rev. B, Condens. Matter*, vol. 60, pp. 5597–5608, 1999.
- [32] M. Bayer, P. Hawrylak, K. Hinzer, S. Fafard, M. Korkusinski, Z. R. Wasilewski, O. Stern, and A. Forchel, "Coupling and entangling of quantum states in quantum dot molecules," *Science*, vol. 291, pp. 451–453, 2001.
- [33] J.-Y. Marzin, J.-M. Gérard, A. Izraël, D. Barrier, and G. Bastard, "Photoluminescence of single InAs quantum dots obtained by self-organized growth on GaAs," *Phys. Rev. Lett.*, vol. 73, pp. 716–719, 1994.
- [34] U. Bockelmann, W. Heller, A. Filoramo, and Ph. Roussignol, "Microphotoluminescence studies of single quantum dots. I. Time-resolved experiments," *Phys. Rev. B, Condens. Matter*, vol. 55, pp. 4456–4468, 1997.
- [35] K. Matsuda, K. Ikeda, T. Saiki, H. Tsuchiya, H. Saito, and K. Nishi, "Homogeneous linewidth broadening in a  $\text{In}_{0.5}\text{Ga}_{0.5}\text{As}/\text{GaAs}$  single quantum dot at room temperature investigated using a highly sensitive near-field scanning optical microscope," *Phys. Rev. B, Condens. Matter*, vol. 63, p. 121 304(R), 2001.
- [36] H. D. Robinson, M. G. Miller, B. B. Goldberg, and J. L. Merz, "Local optical spectroscopy of self-assembled quantum dots using a near-field optical fiber probe to induce a localized strain-field," *Appl. Phys. Lett.*, vol. 72, no. 17, pp. 2081–2083, 1998.
- [37] K. Hinzer, P. Hawrylak, M. Korkusinski, S. Fafard, M. Bayer, O. Stern, A. Gorbunov, and A. Forchel, "Optical spectroscopy of a single  $\text{Al}_{0.36}\text{In}_{0.64}\text{As}/\text{Al}_{0.33}\text{Ga}_{0.67}\text{As}$  quantum dot," *Phys. Rev. B, Condens. Matter*, vol. 63, p. 75 314, 2001.
- [38] H. D. Robinson and B. B. Goldberg, "Light-induced spectral diffusion in single self-assembled quantum dots," *Phys. Rev. B, Condens. Matter*, vol. 61, pp. R5086–R5089, 2000.
- [39] H. T. Johnson, R. Bose, H. D. Robinson, and B. B. Goldberg, "Simulation evidence for lateral excitation transfer in a self-assembled quantum dot array," in *Appl. Phys. Lett.*, to be published.
- [40] Q. Wu, R. D. Grober, D. Gammon, and D. S. Katzer, "Excitons, biexcitons, and electron-hole plasma in a narrow 2.8-nm  $\text{GaAs}/\text{Al}_x\text{Ga}_{1-x}\text{As}$  quantum well," *Phys. Rev. B, Condens. Matter*, vol. 62, pp. 13 022–13 027, 2000.
- [41] E. Dekel, D. Gershoni, E. Ehrenfreund, J. M. Garcia, and P. M. Petroff, "Carrier-carrier correlations in an optically excited single semiconductor quantum dot," *Phys. Rev. B, Condens. Matter*, vol. 61, pp. 11 009–11 020, 2000.
- [42] H. Htoon, D. Kulik, O. Baklenov, A. L. Holmes, Jr., T. Takagahara, and C. K. Shih, "Carrier relaxation and quantum decoherence of excited states in self-assembled quantum dots," *Phys. Rev. B, Condens. Matter*, vol. 63, p. 241 303, 2001.
- [43] L. Novotny, E. J. Sanchez, and X. S. Xie, "Near-field optical imaging using metal tips illuminated by higher-order Hermite-Gaussian beams," *Ultramicroscopy*, vol. 71, pp. 21–29, 1998.
- [44] E. J. Sanchez, L. Novotny, and X. S. Xie, "Near-field fluorescence microscopy based on two-photon excitation with metal tips," *Phys. Rev. Lett.*, vol. 82, pp. 4014–4017, 1999.
- [45] J. Wessel, "Surface-enhanced optical microscopy," *J. Opt. Soc. Amer.*, vol. B2, pp. 1538–1540, 1985.
- [46] Ch. Hafner, *The Generalized Multiple Multipole Technique for Computational Electromagnetics*. Boston, MA: Artech House, 1990.
- [47] L. Novotny, M. R. Beversluis, K. S. Youngworth, and T. G. Brown, "Longitudinal field modes probed by single molecules," *Phys. Rev. Lett.*, vol. 86, pp. 5251–5254, 2001.
- [48] Y. C. Martin, H. F. Hamann, and H. K. Wickramasinghe, "Strength of the electric field in apertureless near-field optical microscopy," *J. Appl. Phys.*, vol. 89, pp. 5774–5778, 2001.
- [49] C. Sönnichsen, T. Franzl, T. Wilk, G. von Plessen, J. Feldmann, O. Wilson, and P. Mulvaney, "Drastic reduction of plasmon damping in gold nanorods," *Phys. Rev. Lett.*, vol. 88, p. 77 402, 2002.
- [50] J. P. Kottmann, O. J. F. Martin, D. R. Smith, and S. Schultz, "Dramatic localized electromagnetic enhancement in plasmon resonant nanowires," *Chem. Phys. Lett.*, vol. 341, pp. 1–6, 2001.
- [51] R. X. Bian, R. C. Dunn, X. S. Xie, and P. T. Leung, "Single molecule emission characteristics in near-field microscopy," *Phys. Rev. Lett.*, vol. 75, pp. 4772–4775, 1995.



**Bennett B. Goldberg** was born in Boston, MA, in 1959. He received the B.A. degree from Harvard College, Cambridge, MA, in 1982, and the M.S. and Ph.D. degrees in physics from Brown University, Providence, RI, in 1984 and 1987, respectively.

Following a Bantrell Postdoctoral appointment at the Massachusetts Institute of Technology and the Francis Bitter National Magnet Lab, he joined the physics faculty at Boston University in 1989. He is currently a Professor of Physics and Professor of Electrical and Computer Engineering. His current research interests include near-field imaging of photonic bandgap, ring microcavity and single-mode waveguide devices; subsurface solid immersion microscopy for silicon inspection; biosensor fabrication and development of waveguide evanescent bioimaging techniques; magneto-optics and magneto-transport of two- and one-dimensional electron systems; and nano-optics of interacting electron systems in quantum wells and quantum-dot structures. He serves as program chair for the Nano-optics subcommittee for the 2002 Quantum Electronics and Laser Science conference in Long Beach, CA, as well as on the program committee for the 7th International Conference on Near-Field Optics.

Dr. Goldberg is a Member of APS, MRS, and LEOS.

**S. B. Ippolito** (M'01), photograph and biography not available at the time of publication.



**Lukas Novotny** received the Ph.D. degree from the Swiss Federal Institute of Technology (ETH), Zurich, Switzerland, in 1996.

He worked with scanning probe techniques since the early stages of scanning tunneling microscopy at the IBM Research Laboratories, Zurich. After spending three years at the Pacific Northwest National Laboratory, he joined the Institute of Optics at the University of Rochester, Rochester, NY, to lead the research group in nanooptics. His research is aimed at understanding and controlling nanoscale systems such as single molecules, quantum dots, or biological proteins by optical means.

**Zhiheng Liu**, photograph and biography not available at the time of publication.



**M. Selim Ünlü** (S'92–M'92–SM'95) was born in Sinop, Turkey, in 1964. He received the B.S. degree in electrical engineering from Middle East Technical University, Ankara, Turkey, in 1986, and the M.S.E.E. and Ph.D. degrees in electrical engineering from the University of Illinois, Urbana-Champaign, in 1988 and 1992, respectively. His dissertation topic dealt with resonant cavity enhanced (RCE) photodetectors and optoelectronic switches.

In 1992, he joined the Department of Electrical and Computer Engineering, Boston University, Boston, MA, as an Assistant Professor, and he has been an Associate Professor since 1998. From January to July 2000, he was a Visiting Professor at the University of Ulm, Germany. His career interest is in research and development of photonic materials, devices, and systems focusing on the design, processing, characterization, and modeling of semiconductor optoelectronic devices, especially photodetectors. He has authored and co-authored more than 150 technical articles and several book chapters and magazine articles; edited one book; holds one U.S. patent; and has several patents pending.

Dr. Ünlü served as the Chair of IEEE Laser and Electro-Optics Society, Boston Chapter, during 1994–1995, winning the LEOS Chapter-of-the-Year Award. He served as the vice president of SPIE New England Chapter in 1998–1999. He was awarded the National Science Foundation Research Initiation Award in 1993, the United Nations TOKTEN award in 1995 and 1996, and both the National Science Foundation CAREER and Office of Naval Research Young Investigator Awards in 1996. During 1999–2001, he served as the chair of the IEEE/LEOS technical subcommittee on photodetectors and imaging, and he is currently an Associate Editor for IEEE JOURNAL OF QUANTUM ELECTRONICS.